

## A petrological approach to the study of ancient glass

BRUNO MESSIGA<sup>1\*</sup> and M. PIA RICCARDI<sup>2</sup>

<sup>1</sup> Dipartimento di Scienze della Terra, Università di Pavia, Via Ferrata 1, I-27100 Pavia, Italy  
CNR - Centro Studi per la Cristallografia e la Cristallografia (CSCC), Via Ferrata 1, I-27100 Pavia, Italy

<sup>2</sup> Centro Grandi Strumenti (CGS) - Università di Pavia, Via A. Bassi 21, I-27100 Pavia, Italy

Submitted, September 2000 - Accepted, February 2001

**ABSTRACT.** — In glass archaeology, «production indicators» are those remains which testify to specific operations carried out during the productive cycle; they allow us to reconstruct the processes and technological expedients used in the past to produce glass. The intermediate products of glass melting reveal textural and chemical inhomogeneities which may be used to infer parts of the production history. Samples of glass masses belonging to an early stage of glass making were unearthed in the archaeological sites of Lomello (province of Pavia, Italy) (I-IV centuries A.D.) and Val Gargassa (Genova) (late XII Century A.D.). In these materials, unmelted mineral phases, banded textures, phase separation, and crystallisation all produce different textures which supply information on: provenance of raw materials; components added and the efficiency of the melting process; liquid immiscibility and refining processes; cooling rate of vitreous products.

The composition of glass influences the different arrangements of tetrahedral-fold cations ( $\text{SiO}^{4-}$ ,  $\text{AlO}^{3-}$ ) and determines the various properties and features of the glass itself. The low effective diffusivity prevents the composition from becoming homogeneous during glass melting, and consequently evidence of early production steps is retained.

Mineral relics present in the micro-textures of

glassy materials (i.e., fining slags) have great archaeometric value, because they may indicate the provenance of raw materials. The composition of relic mineral phases also supplies important analytical grounds on which to define the recipes followed during glass making, in terms of vitrifying, stabilising, flushing and additive components.

**RIASSUNTO.** — Nella archeologia del vetro gli «indicatori di produzione» sono dei reperti che testimoniano certe operazioni svolte durante il ciclo produttivo. Questi prodotti intermedi della lavorazione hanno caratteristiche tessiture e composizionali che permettono di risalire agli espedienti tecnologici usati nella produzione.

I campioni studiati appartengono agli stadi iniziali del ciclo di lavorazione del vetro e sono stati rinvenuti nei siti archeologici di Lomello (in provincia di Pavia, I-IV secolo d.C.) e in Val Gargassa (in provincia di Genova, tardo XII secolo d.C.).

In tali materiali sono abbondanti fasi cristalline non completamente fuse, tessiture a bande, cristallizzazione di fasi ed evidenze di immiscibilità tra fusi. Tale varietà di tessiture può fornire informazioni sulla provenienza della miscela vetrificabile, sui componenti usati e sulla efficienza del processo di fusione. Inoltre, può essere pure usata per interpretare le cause della immiscibilità tra le fasi fuse e le loro relazioni con il processo di raffinazione della pasta vitrea come pure fornire valutazioni sulla velocità del processo di raffreddamento. La

\* Corresponding author, E-mail: messiga@crystal.unipv.it

composizione del vetro influenza in modo significativo la disposizione dei cationi a coordinazione tetraedrica ( $\text{SiO}_4^-$ ,  $\text{AlO}_3^-$ ) determina quindi le differenze nelle proprietà e caratteristiche del vetro. La bassa diffusività all'interno della massa fusa impedisce la omogeneizzazione composizionale; di conseguenza sono conservate le evidenze di vari momenti della lavorazione. I minerali relitti ritrovati nelle microstrutture di materiali quali sono le scorie di schiumatura hanno un elevato valore archeometrico, perchè possono fornire gli elementi per risalire alla provenienza delle materie prime. Pure i minerali presenti come relitti non completamente fusi costituiscono la base per ricostruire le ricette utilizzate nella produzione del vetro, in termini di componenti vetrificanti, stabilizzanti, fondenti ed additivi.

KEY WORDS: *Northern Italy, glass, archaeometry, microanalysis, production indicators, petrology.*

## INTRODUCTION

Glass making is an extremely old technology, the history of which has often been recounted. The earliest written records of glass making are the famous clay tablets, dated around 650 B.C., from the library of Assurbanipal (Newton, 1980). Frit and glass cakes are reported to have been produced in so-called «primary workshops» in Eastern countries (Foy and Jézégou, 1996, 1997), where the first stages of glass production (glass making) were carried out. The glass cakes (ingots) were sent to «secondary workshops» where a further stage (glass melting) was accompanied by a fining process leading to worked glass production. It is thought that glass making technology was not entirely transferred to Western countries until Medieval times (Foy *et al.*, 1998, and refs. therein). Glass is an artefact the making of which requires advanced technology in terms of selection of raw materials, so that firing also had to have reached good efficiency levels. In addition to the considerable energy involved, glass making requires flushing components, which contribute towards lowering the melting temperature (Sternini, 1995; Mannoni and Giannichedda, 1996, and refs. therein; Newton and Davidson, 1997). From the frit, a preliminary raw glass

(which cannot be worked because it is only partially melted), to worked glass, several steps must be carried out, which basically modify the intrinsic characters of the earlier raw glass by means of additive components. Recycling of used glass (cullets) was a commonly used expedient (Sternini, 1995).

In glass archaeology, the so-called «production indicators» are those remains which testify to specific operations carried out during the productive cycle, implying fritting, melting, mixing, boiling and working. In other words, they allow us to reconstruct the processes and technological expedients used in the past to produce glass. For the sake of simplicity, they may be divided into two groups: 1) *indicators closely related to glass production*: raw materials (sand, quartz-rich rock, ash), intermediate products (frits), production waste (scum, cuttings, fluidity tests, transparent and opaque glass masses, collars, drippings); 2) *indicators indirectly related with production*: kiln conduction (temperature, redox) and construction materials (stone, mortar bricks), tools (crucibles, metal tools) and fuel (charcoal) (Mendera, 2000, pers. comm.).

Until now, archaeometric studies have mainly been carried out by comparing bulk chemical characters, in order to infer age and provenance attributes (Nenna *et al.*, 1997; Foy *et al.*, 1998; Gratuze *et al.*, 1998). Apart from studies on surface alterations (Libourel *et al.*, 1997; Schvoerer *et al.*, 1997), textural and compositional studies on heterogeneity are lacking. Only recently have the relationships between micro-textures and micro-analyses been envisaged as potential criteria to define technological expedients used in a given productive cycle (Giannichedda *et al.*, 2000).

Modern theories such as the «random network hypothesis» (Zachariasen, 1932), «phase separation structure» (Uhlmann and Kolbeck, 1976) and «strained cluster model» (Goodman, 1986) have demonstrated the intrinsically inhomogeneous nature of glass. On these bases, the study of inhomogeneities in glass is an important tool to understand present-day and ancient glass-making technology.

This paper aims at demonstrating that inhomogeneities within ancient glass samples can record phases of production history. The textural and chemical inhomogeneities of various glasses are described, analysed and interpreted. Materials not matching the definition of the «essentially homogeneous nature of glass» were selected and *in situ* microprobe analyses were performed on phases in relevant micro-textures. The samples do not represent worked glass (finished artefacts) but glass masses suitable for further processing (unfinished products) and consequently definable as «production indicators».

#### MATERIALS AND METHODS

Sampled materials were unearthed in the archaeological sites of Lomello (Pavia) (Blake and Maccabruni, 1985; Blake *et al.*, 1987) and Val Gargassa (Genova) (Giannichedda, 1992, 1997). Table 1 summarizes their features.

Textures reveal the presence of various glass types, even within a single sample, and crystalline phases.

*Vitreous masses* and *glass cake* are massive samples composed of coloured glass. The former are glass fragments of variable size which represent either unfinished products or material for mosaic *tesserae*; the latter is a particular type of round glass ingot. Both types display a ribbon texture dominated by alternating pale (yellowish) and darker (reddish-brown) bands. The thicker bands contain transparent glassy portions (colourless), rounded to elongated in shape, with diffuse bubbles and lesser ductile behaviour than adjacent bands. Some of the darker bands, of variable thickness, show a subparallel trend with a fluidal aspect and folding. The bands become thicker near the fold hinges. Small isolated masses of darker glass may also be found within the ribbon texture. Crystalline phases and inhomogeneities are widespread.

TABLE 1  
*Examined materials.*

| Typology                      | Provenance / Age                         | Contest         | Texture and Mineralogy  |
|-------------------------------|--|-----------------|---|
| vitreous mass<br>US3358B      | Lomello (PV)<br>I-IV century AC          | housing contest | <ul style="list-style-type: none"> <li>• ribbon, folded texture</li> <li>• transparent glass portions, with rounded to elongated shape</li> <li>• quartz relics</li> <li>• metallic inclusions</li> </ul> |
| vitreous mass<br>US2<br>VGR9  | Val Gargassa (GE),<br>end of XII century | workshop        | <ul style="list-style-type: none"> <li>• ribbon, folded texture</li> <li>• feldspar relics</li> <li>• quartz relics</li> <li>• diopside</li> </ul>  |
| glass cake<br>VM1219/1        | Lomello, no age                          | housing contest | <ul style="list-style-type: none"> <li>• ribbon, folded texture</li> <li>• feldspar relics</li> <li>• quartz relics</li> <li>• crystallisation of akermanite, wollastonite</li> </ul>                     |
| vitreous mass<br>US1<br>VGR11 | Val Gargassa,<br>end of XII century      | workshop        | <ul style="list-style-type: none"> <li>• ribbon texture</li> <li>• crystallisation of wollastonite</li> <li>• and zoned diopside</li> </ul>   |
| fining slag<br>US3303B        | Lomello, Late<br>Medieval                | housing contest | <ul style="list-style-type: none"> <li>• mineral relics from batch</li> <li>• skeletal growth of crystals</li> </ul>  |

*Fining slags* are vesicular textured, generally dark-brown fragments, which represent scums produced during glass boiling, retaining the impurities of the glass melt and skimmed from the surface contents of crucibles. The bubbles do not exceed 5 mm in diameter and have a gently elongated shape. Also abundant are smaller microbubbles (up to 10  $\mu$ m). Metallic inclusions are rare. Crystalline phases are widespread, and represent either relic (refractory) phases or minerals nucleated during cooling of the vitreous material.

Samples were thin-sectioned and then analysed. Spot data were necessary for *in situ* chemical analysis of phases related to particular microtextures. An electron microprobe (EMP) was used to perform *in situ*

micro-analyses (Tables 2, 3, 4) on polished thin sections. Microtextural examination under optical (OM) and scanning electron (SEM) microscopes was also essential. This analytical strategy was applied using equipment in the CSCC and CGS laboratories of the University of Pavia.

Micro-analyses were performed on a JEOL JXA 840A electron analyser equipped with three wavelength-dispersive spectrometers (WDS) (TAP, PET, LIF analysing crystals) and one Si(Li) energy-dispersive spectrometer (Be-window). Analytical conditions were 20kV accelerating voltage and 20 nA. Spot size was 5  $\mu$ m. Counting time was 20 seconds for all elements except Mn and Fe (40 sec.). Data collected by the WDS were processed with the TASK correction program. Mineral phases

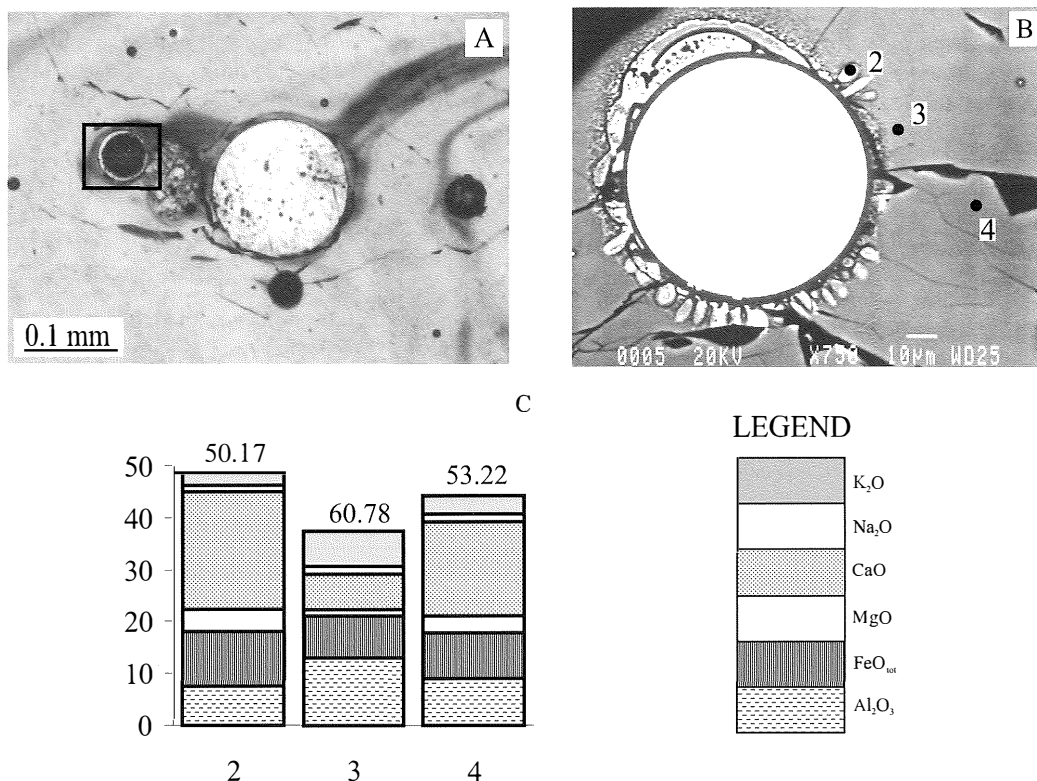


Fig. 1— Immiscibility in vitreous masses. A: OM texture between glass, gas (coarse, paler) and Fe-P phase (small, darker). B: SEM image, showing a detail of Fe-P phase and finger-like rim; numbers are *in situ* analysis positions. C: Histogram showing relevant compositions of different spots on B; see numbers. Data in wt% oxide.  $SiO_2$  is number at tip of each bar.

TABLE 2

*Lomello vitreous mass (Figures 1 and 2, sample US3358B); Lomello glass cake (Figure 3, VM1219/1);  
Val Gargassa vitreous masses (Figures 4 and 5, US1/VGR11, US2/VGR9).*

|                                | Figure 1 |        |        |        | Figure 2 |        |       |          | Figure 3 |        |        |        |        |       |
|--------------------------------|----------|--------|--------|--------|----------|--------|-------|----------|----------|--------|--------|--------|--------|-------|
|                                | 2        | 3      | 4      | Fe-P   | 2        | 6      | 8     | 9        | 20       | 21     | 43     | 53     | 48     | 51    |
| SiO <sub>2</sub>               | 50.17    | 60.78  | 53.22  | 0.00   | 64.24    | 51.93  | 55.23 | 51.37    | 64.38    | 51.19  | 51.45  | 47.81  | 52.07  | 43.29 |
| TiO <sub>2</sub>               | 0.58     | 0.27   | 0.44   | 0.00   | 0.05     | 0.58   | 0.53  | 0.62     | 0.03     | 0.30   | 0.08   | 0.39   | 0.06   | 0.00  |
| Al <sub>2</sub> O <sub>3</sub> | 7.62     | 13.06  | 9.14   | 0.00   | 19.47    | 9.79   | 10.04 | 9.57     | 18.34    | 4.89   | 4.58   | 5.72   | 0.08   | 2.21  |
| Cr <sub>2</sub> O <sub>3</sub> | 0.70     | 0.05   | 0.00   | 0.00   | 0.06     | 0.00   | 0.01  | 0.01     | 0.00     | 0.00   | 0.00   | 0.03   | 0.00   | 0.00  |
| FeO <sub>tot</sub>             | 10.57    | 8.00   | 8.66   | 86.19  | 0.07     | 9.06   | 7.94  | 9.53     | 0.05     | 2.19   | 0.87   | 2.46   | 0.06   | 1.01  |
| MnO                            | 0.57     | 0.17   | 0.50   | 0.00   | 0.00     | 0.49   | 0.42  | 0.53     | 0.03     | 0.06   | 0.05   | 0.15   | 0.01   | 0.11  |
| MgO                            | 4.20     | 1.37   | 3.41   | 0.00   | 0.01     | 3.43   | 2.91  | 3.41     | 0.00     | 4.81   | 2.57   | 6.13   | 0.00   | 12.62 |
| CaO                            | 22.47    | 6.67   | 18.11  | 0.00   | 0.23     | 17.14  | 14.48 | 17.76    | 0.26     | 14.33  | 34.08  | 17.67  | 48.28  | 39.06 |
| Na <sub>2</sub> O              | 1.27     | 1.64   | 1.30   | 0.00   | 2.10     | 1.78   | 1.84  | 1.82     | 0.00     | 1.20   | 0.02   | 0.55   | 0.00   | 0.24  |
| K <sub>2</sub> O               | 2.50     | 6.64   | 3.58   | 0.00   | 13.10    | 3.86   | 4.79  | 3.48     | 16.89    | 19.18  | 6.30   | 19.09  | 0.17   | 1.43  |
| Cl                             | 0.00     | 0.00   | 0.00   | 0.00   | 0.00     | 0.00   | 0.00  | 0.00     | 0.00     | 0.00   | 0.00   | 0.00   | 0.00   | 0.00  |
| P <sub>2</sub> O <sub>5</sub>  | 0.00     | 1.80   | 1.83   | 13.81  | 0.00     | 1.93   | 1.80  | 1.91     | 0.00     | 2.38   | -      | -      | -      | -     |
| Tot wt%                        | 100.65   | 100.45 | 100.19 | 100.00 | 99.33    | 99.99  | 99.99 | 100.01   | 99.98    | 100.83 | 100.00 | 100.00 | 100.73 | 99.97 |
|                                | Figure 4 |        |        |        |          |        |       | Figure 5 |          |        |        |        |        |       |
|                                | 129      | 130    | 134    | 131    | 132      | 133    | 167   | 168      | 169      | 170    | 171    |        |        |       |
| SiO <sub>2</sub>               | 49.01    | 50.80  | 55.23  | 52.02  | 54.28    | 55.95  | 67.76 | 66.46    | 73.57    | 72.78  | 77.37  |        |        |       |
| TiO <sub>2</sub>               | 0.45     | 0.30   | 0.40   | 0.30   | 0.24     | 0.38   | 0.00  | 0.00     | 0.22     | 0.19   | 0.15   |        |        |       |
| Al <sub>2</sub> O <sub>3</sub> | 2.97     | 2.13   | 1.86   | 2.17   | 1.68     | 6.00   | 19.39 | 19.52    | 4.72     | 4.86   | 3.91   |        |        |       |
| Cr <sub>2</sub> O <sub>3</sub> | 0.00     | 0.00   | 0.00   | 0.00   | 0.00     | 0.00   | 0.00  | 0.00     | 0.00     | 0.00   | 0.00   |        |        |       |
| FeO <sub>tot</sub>             | 14.20    | 11.24  | 1.07   | 8.64   | 4.63     | 12.80  | 0.00  | 0.00     | 1.08     | 0.88   | 0.70   |        |        |       |
| MnO                            | 0.00     | 0.00   | 0.00   | 0.00   | 0.00     | 0.04   | 0.00  | 0.00     | 0.00     | 0.00   | 0.00   |        |        |       |
| MgO                            | 10.31    | 12.03  | 17.06  | 13.24  | 15.31    | 3.58   | 0.00  | 0.00     | 2.85     | 2.77   | 2.04   |        |        |       |
| CaO                            | 19.17    | 20.21  | 23.16  | 20.45  | 22.45    | 7.76   | 0.08  | 0.46     | 5.13     | 5.07   | 3.84   |        |        |       |
| Na <sub>2</sub> O              | 2.64     | 2.23   | 1.03   | 2.03   | 1.05     | 9.34   | 9.54  | 8.54     | 8.65     | 9.70   | 8.38   |        |        |       |
| K <sub>2</sub> O               | 0.17     | 0.13   | 0.13   | 0.15   | 0.12     | 3.26   | 3.21  | 4.72     | 2.92     | 2.81   | 2.89   |        |        |       |
| Cl                             | 0.21     | 0.21   | 0.18   | 0.20   | 0.18     | 1.04   | 0.00  | 0.30     | 0.86     | 0.96   | 0.80   |        |        |       |
| P <sub>2</sub> O <sub>5</sub>  | 0.00     | 0.00   | 0.00   | 0.00   | 0.00     | 0.00   | 0.00  | 0.00     | 0.00     | 0.00   | 0.00   |        |        |       |
| Tot wt%                        | 100.17   | 100.18 | 100.18 | 100.01 | 100.18   | 100.15 | 99.98 | 100.00   | 100.00   | 100.02 | 100.08 |        |        |       |

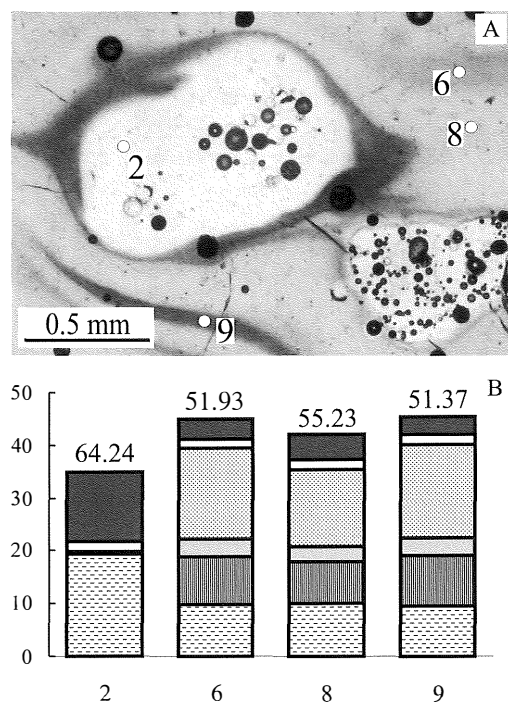


Fig. 2 – A: Microtexture (OM) showing pale glass portions (bubble-filled), surrounded by darker glass shadows. Vitreous mass has ribbon texture. Numbers are analytical. B: Histogram of various spot analyses; details as in fig 1.

were used as standards. Estimated precision was about 3% for major and 10% for minor elements, respectively.

#### MICROTEXTURES AND RELATED COMPOSITIONS

Within the glass samples, microtextures mainly revealed so-called «defects», i.e., unmelted mineral relics of raw materials, inhomogeneities during melting, devitrification products and gas inclusions (bubbles).

In the vitreous mass (Lomello, sample US3358B) some dark, perfectly rounded inclusions about 100 mm in diameter were observed. Under the optical microscope (transmitted light), they turned out to be

opaque and generally armoured by a transparent rim a few tens of microns wide, strongly contrasting in colour with the yellowish-brown vitreous mass. In figs. 1A and 1B, they are shown together with larger gas inclusions. The rounded shape of the inclusions reveals phase immiscibility and the physical nature of the process, dominated by an arrangement of phase boundaries controlled by surface tension in a liquid medium. Under the electron microscope, the dark inclusions showed a homogeneous aspect as a consequence of their constant chemical composition. The rims are mainly composed of finger-like fassaitic clinopyroxene (about 10 mm wide) radiating within the glass body perpendicularly to the inclusion surface. The composition of the inclusions (Table 2) reveals the presence of a P-Fe alloy (average P/Fe ratio 0.16). The physical state of the inclusions (i.e., crystalline or amorphous) is still unknown. Around the inclusions, the composition of the glass changes considerably (fig. 1C): higher  $\text{SiO}_2$ ,  $\text{Al}_2\text{O}_3$  and  $\text{K}_2\text{O}$  and lower CaO are retained by the glass nearest to the clinopyroxene (Table 2). Moving away from the inclusions, the compositional gradients are very sharp (i.e., 0.2 wt%/mm for  $\text{SiO}_2$ ).

The ribbon texture of the vitreous mass (fig. 2A) indicates that compositionally distinct melts flowed, some more readily than others. In particular, the lighter glass portions (filled with bubbles) indicate a melt with very high viscosity. *In situ* analyses of various bands reveal clearcut differences in terms of vitrifying/stabilising components (fig. 2B).  $\text{SiO}_2$  and  $\text{Al}_2\text{O}_3$  (vitrifying) contents are higher in the brownish portions, which are more viscous than the yellowish ones, which in turn contain higher CaO, MgO and FeO (stabilising) contents. The chemistry of the paler glass matches the composition of K-feldspar, with appreciable  $\text{NaK}_1$  substitution (Table 2).

Compositionally clearly defined phases occur in glass cake (Lomello, sample VM1219/1) (fig. 3). They are considered to be «devitrification phases» and are currently interpreted as crystallisation products of glass.

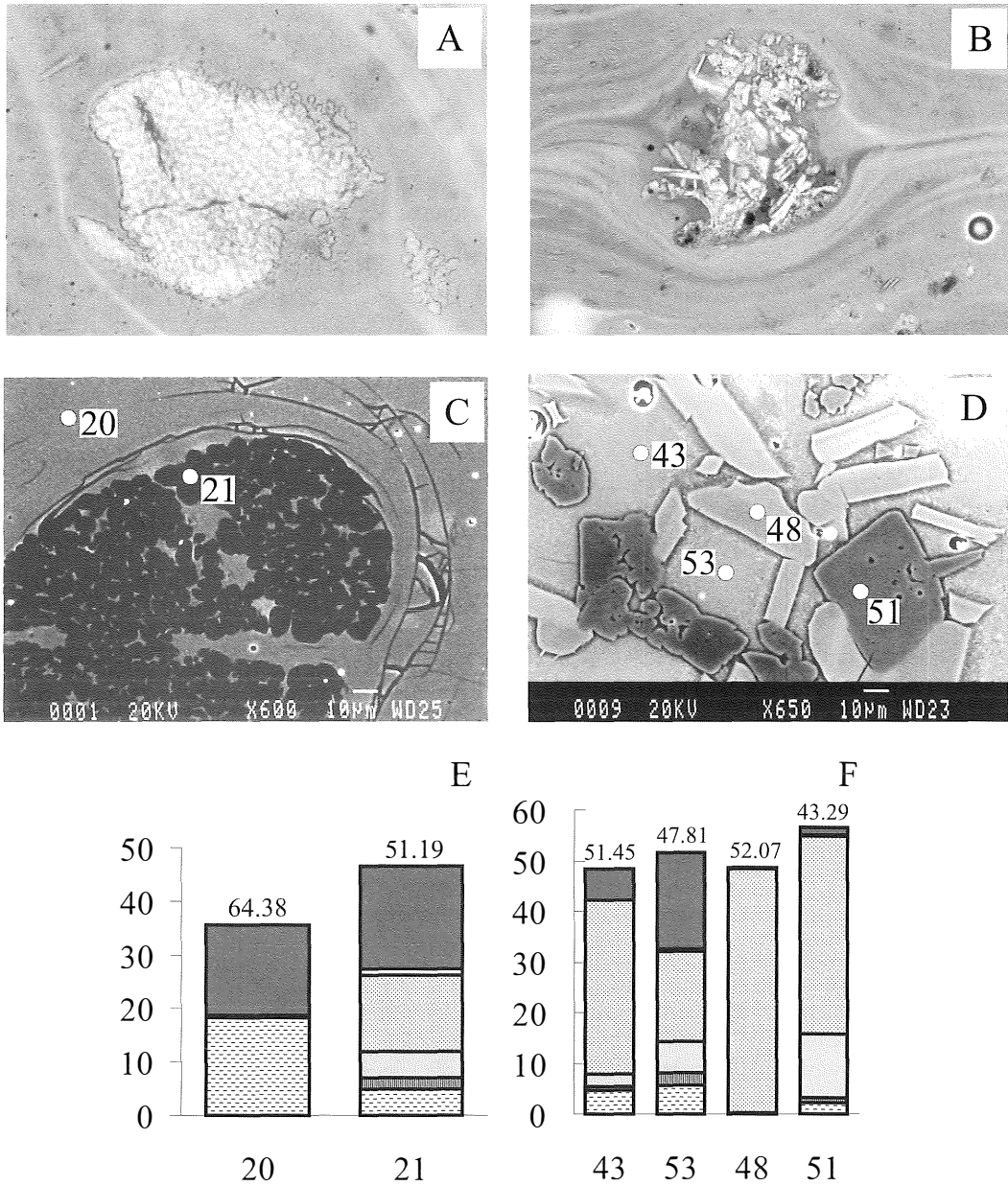


Fig. 3 – Microtextures of «devitrification phases» under OM (A, B) and EM (BSE) microscopes (C,D). A and C: aggregates of rounded particles; B and D: euhedral diopside (paler) and akermanite (darker) crystals. E and F: histograms of phase compositions from both textures; details as in fig 1.

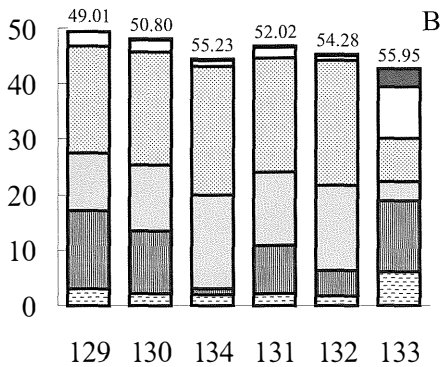
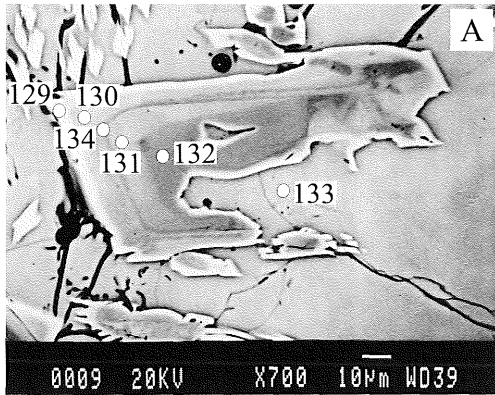


Fig. 4 – Zoned clinopyroxene. A: BSE image reveals oscillatory zoning and reports spot positions. B: Histogram showing various compositions; details as in fig 1.

Microtextural examination distinguished two different types of inclusions: i) aggregates of euhedral crystals (figs. 3B, 3D); ii) aggregates of rounded particles (figs. 3A, 3C). The former are akermanite and wollastonite, birefringent under the optical microscope (crossed polarised light); the latter are compositionally similar to K-feldspar and not birefringent (Table 2). The glass nearest to the rounded-grain aggregates have high  $K_2O$  contents (up to 19.18 wt%). The aggregates of wollastonite and akermanite are compositionally unzoned and formed by direct segregation from the melt. Glass composition changes accordingly: within the aggregates it is lower in CaO and  $SiO_2$  (17.67 and 47.81 wt%,

respectively) than outside them (34.08 wt% CaO and 51.45 wt%  $SiO_2$ ).

Diopside crystals within vitreous masses (Val Gargassa, sample US1-VGR11) reveal oscillatory zoning and reabsorption phenomena by the melt (figs. 4A, 4B). Zoning is controlled by Fe/Mg substitution. Pyroxene also displays appreciable amounts of  $Na_2O$  (up to 2.64 wt%) owing to the alkaline character of the melt (9.34 wt%  $Na_2O$ ) (Table 2).

Evidence of the mineral composition of batch mixtures is revealed by mineral relics and particular glass compositions. In the vitreous mass shown in fig. 5A (Val Gargassa, sample

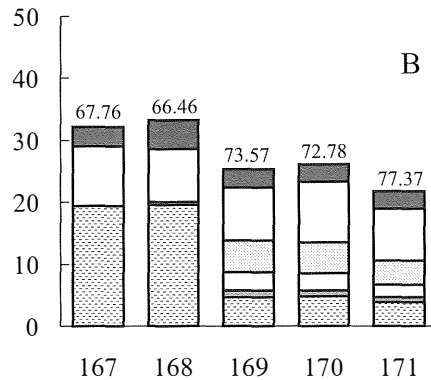
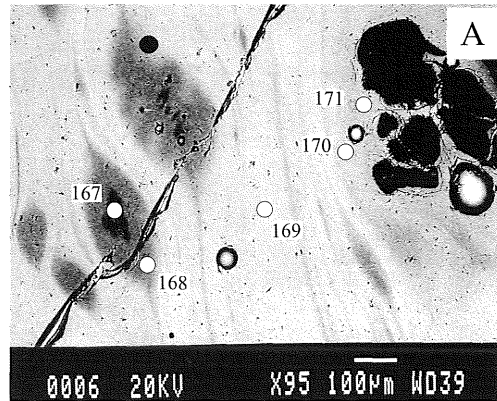


Fig. 5 – Mineral relics in vitreous mass. A: embayed quartz relics (dark; upper right corner) and relics of feldspar with elongated shape and evident zoning (left) within a banded glass mass (OM). Numbers are spot analysis positions. B: histogram with spot compositions; details as in fig 1.



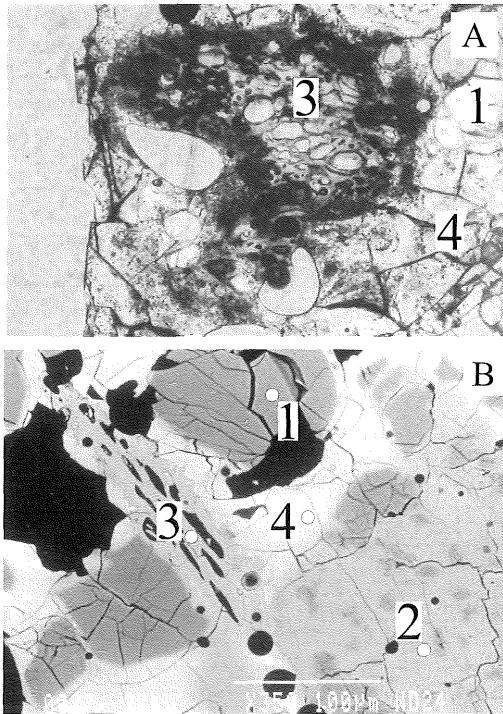


Fig. 6 – Microtexture of vitreous slag showing relics of batch minerals, under OM (A) and BSE (B) microscopes. 1: quartz, 2: feldspar, 3: mica, 4: glass.

US2-VGR9), the microtexture coupled with spot analyses reveals the presence of a crystalline  $\text{SiO}_2$  phase (quartz), together with lenticular domains in which relic feldspar occurs. The nearest glass also matches feldspar composition (Table 2). Quartz displays embayment due to partial reabsorption by the melt; strong compositional zoning is induced in the nearest glass portions.  $\text{K}_2\text{O}$  contents rapidly decrease from core to rim of the lenticular domains (from 3.21 to 4.72  $\text{K}_2\text{O}$  wt%) (fig. 5B). The highest  $\text{SiO}_2$  contents in glass occur near the quartz boundary ( $\text{SiO}_2$  up to 77.37). Within the groundmass,  $\text{SiO}_2$  and  $\text{K}_2\text{O}$  are 73.57 and 2.92 wt%, respectively (Table 2).

The texture of fining slag (Lomello, sample Us3303B) (figs. 6A, 6B) reveals the presence of refractory minerals, probably derived from the batch: quartz, feldspars, micas, Mg-olivine,

spinel, zircon, rutile, sillimanite and apatite. They display evident embayment of crystal rims due to reactions with the melt. In particular, mica is converted into an amorphous phase, with trails of small bubbles oriented along the mineral cleavage planes. Instead, phases such as diopside and wollastonite crystallised during glass cooling. Skeletal Mg-olivine appears along the rims of Mg-olivine relics.

## DISCUSSION

The above data allow us to discuss several points such as glass making technology, and the reasons for glass immiscibility and crystalline phase separation.

### *Glass making*

The examined samples retain several unmelted mineral relics of the batch. It is well-known that early glass making and melting processes were carried out in two different and distant regions (Foy *et al.*, 1998). Moreover, for many ancient peoples, glass making was a highly esoteric operation which had to be conducted on a propitious day and in a favourable month (Oppenheim *et al.*, 1970).

Some aspects concerning the thermal properties of the batch may explain this cautious approach to glass making. At the same temperature, the overall thermal conductivity of the batch is lower than that of glass (Cable, 1991). Historical sources indicate that Assyrian recipes insist on the fact that sand and plant ash mixtures must be heated together for a long time at a dull red heat (Newton, 1980). A recent experimental archaeology run (Jackson *et al.*, 1998) indicates that the melting time for an ash-sand mixture is 24 hours at 1390°. It is essential for all batch components to be in contact with each other, and good contact cannot be guaranteed until some liquid has formed and is able to percolate around solid grains. The temperature of eutectic melting occurring at solid surfaces among phases is

constrained by the number of crystalline phases involved. As a rule, eutectic temperature decreases as the number of phases increases. It is reasonable to imagine that early melts corresponded to a eutectic temperature with a low number of phases, because reciprocal contact among all phases hardly ever occurs. When this first liquid percolates, it amplifies chemical communications among whole grains; consequently, melting temperature rapidly decreases and melting rate increases. A «magic» expedient used to obtain an early liquid able to reduce the melting temperature was to add cullet to the batch (Sternini, 1995). The melting of a non-crystalline phase, such as glass, causes the onset of melting of the whole batch at lower temperatures. In ancient and present-day production, frit commonly contains recycled glass, and this fact has important implications on the temperature of batch melting.

#### *Glass immiscibility*

The inhomogeneity of vitreous masses may be caused by differing viscosity, due to different glass compositions and polymerisation patterns. In igneous petrology, mingling produces a heterogeneous mixture containing discrete portions of the end-member magmas. Each rock portion retains the chemical imprint of its source magma. Similarly, compositional changes in a glass melt produce comparable textures and chemical inhomogeneities, so that the melt varies greatly in density, viscosity and reactivity.

Following Zachariassen's (1932) theory, melt viscosity is directly related to the ratio between network-forming and network-modifying cations, which correspond respectively to vitrifying ( $\text{SiO}_2$ ,  $\text{Al}_2\text{O}_3$ ) and stabilising/flushing ( $\text{CaO}$ ,  $\text{MgO}$ ,  $\text{FeO}$ ,  $\text{K}_2\text{O}$ ,  $\text{Na}_2\text{O}$ ) components. The effective diffusivity values for mass transfer depend to a great extent on both composition and temperature; values do not often exceed  $10^{-10}\text{m}^2\text{s}^{-1}$  (Cable, 1991). Unaided diffusion requires extremely long times to homogenise a viscous liquid. Accordingly, a

glass may be defined as a non-equilibrium material, the inhomogeneities of which may be evidenced on different observational scales; this implies that differences in thermal expansion can considerably increase internal stresses as the glass cools and may make it very fragile at room temperature. Ancient glass unearthed or employed as stained glass often displays inhomogeneous alteration patterns, and the influencing factors are due to different ratios among network-forming and -modifying cations (Newton, 1980).

Subliquidus immiscibility is obvious in vitreous masses because of textural evidence of physical separation among glass, gas and metallic phases. Gases evolve during melting (Cable, 1991). Most of the gas is  $\text{CO}_2$  from carbonates and produces vigorous melt boiling. The consequent refining of glass produces the scum which contains most of the refractory phases (and gases).

In glass paste, the presence of the Fe-P phase is certainly related to the addition of phosphorus. The literature describes phosphorus as an opacifying agent, used to make slightly translucent glass and added in the form of plant ash or bones (Moretti and Moretti, 1998). A non-negligible effect of the addition of phosphorus to a silicate melt is the formation of two distinct and immiscible liquids. In the petrological literature (Roedder, 1979), the occurrence of two conjugate liquids, one Fe- and P-rich and silica-poor, and the other the opposite, is clearly revealed by melting experiments. The latter aspect indicates that the addition of phosphorus during glass melting may play a double role as opacifier and decolouriser. The decolourising process implies that iron may be removed from the molten glass as a Fe-P phase.

#### *Crystalline phase separation*

Phase crystallisation is controlled by the under-cooling rate of melted glass. In the samples examined here, growth is controlled by kinetics; crystal growth may be limited by the rate of transport of heat fusion away from the

interface. In multi-component systems, such as glasses or geo-materials, the limiting step is the diffusion of solute. As growth proceeds, the concentration of the rejected solute at the growth interface increases in thickness, so that diffusion must occur over greater distances and consequently the growth rate ( $u$ ) decreases with time ( $t$ ) according to:

$$u \propto t^{-1/2}$$

Once a diffusion layer has formed, if any perturbation of the equilibrium occurs, the growing interface enters a region where under-cooling is greater, thus accelerating growth. This situation is called constitutional super-cooling (Chalmers, 1964). Dendritic or spherulitic morphologies are typical. In the examined samples, dendritic growth is displayed by phases growing into slag, due to high under-cooling.

The textural and chemical features of inclusions in vitreous masses allow us to draw various conclusions. The first type (rounded particles) may be a raw material partially dissolved in the glass during its making, whereas wollastonite and akermanite crystals may be considered as true devitrification phases, representing the onset of crystallisation within a slowly cooled melt. The presence of zoned clinopyroxene provides new insight into crystallisation dynamics occurring in melted glass masses. Although the FeO/MgO ratio increases from core to rim, according to a normal crystallisation pathway, oscillatory zoning indicates poor diffusion of components within the melt during diopside crystallisation and an alternate concentration of rejected solute as crystallisation proceeds.

The presence of relic rounded particles (within glass cake) matching feldspar composition, opens the question as to whether ash is an alkali carrier or not in glass making. Although the compositions of relics do indicate the presence of natural feldspar in the batch, the current literature suggests that the use of plant ash is to supply fluxing components to

the glass (Jackson *et al.*, 1998, and refs. therein). The vitreous mass from Val Gargassa shows relics of a K-feldspar mineral phase, probably occurring within the batch. In the presence of Al<sub>2</sub>O<sub>3</sub> and SiO<sub>2</sub>, the potash from ash reacts to form a K-silico-alluminate, as shown by analysis of the liquidus and subliquidus surfaces of the KAS (K<sub>2</sub>O–Al<sub>2</sub>O<sub>3</sub>–SiO<sub>2</sub>) system (fig. 7). The glass cake composition indicates the occurrence of peritectic reactions, yielding a melt and a feldspar phase. However, the temperatures at which the process occurs, although dependent on composition, are higher than 695°C.

Abundant relic minerals (refractory phases) contained in the fining slags from Lomello indicate the use of a raw sandy material which had not been completely purified. Mineral phases such as micas, olivine, zircon, spinel, ilmenite, sillimanite and quartz may give insights into the provenance of this sand. All the mineral phases in the fining slags are closely comparable with mineral phases found in Roman bricks and tiles from the Lomello production site (Cairo, 1998; Cairo *et al.*, 2001/submitted), strongly suggesting that glass was produced locally in the Lomello area, at least in Medieval times (cf. Table 1 for age details).

## CONCLUSIONS

As well as provenance attributes, based on the presence of relic minerals and compositions, several other technological attributes result when glass inhomogeneities are considered. Moreover, in archaeology studies regarding production, scientific analyses allow direct inferences on the reconstruction of glass making and melting history. This may occur, for example, when semi-finished products or glassy materials were intentionally discarded from the production cycle at a given moment in time, and are later investigated.

Glass composition influences the different

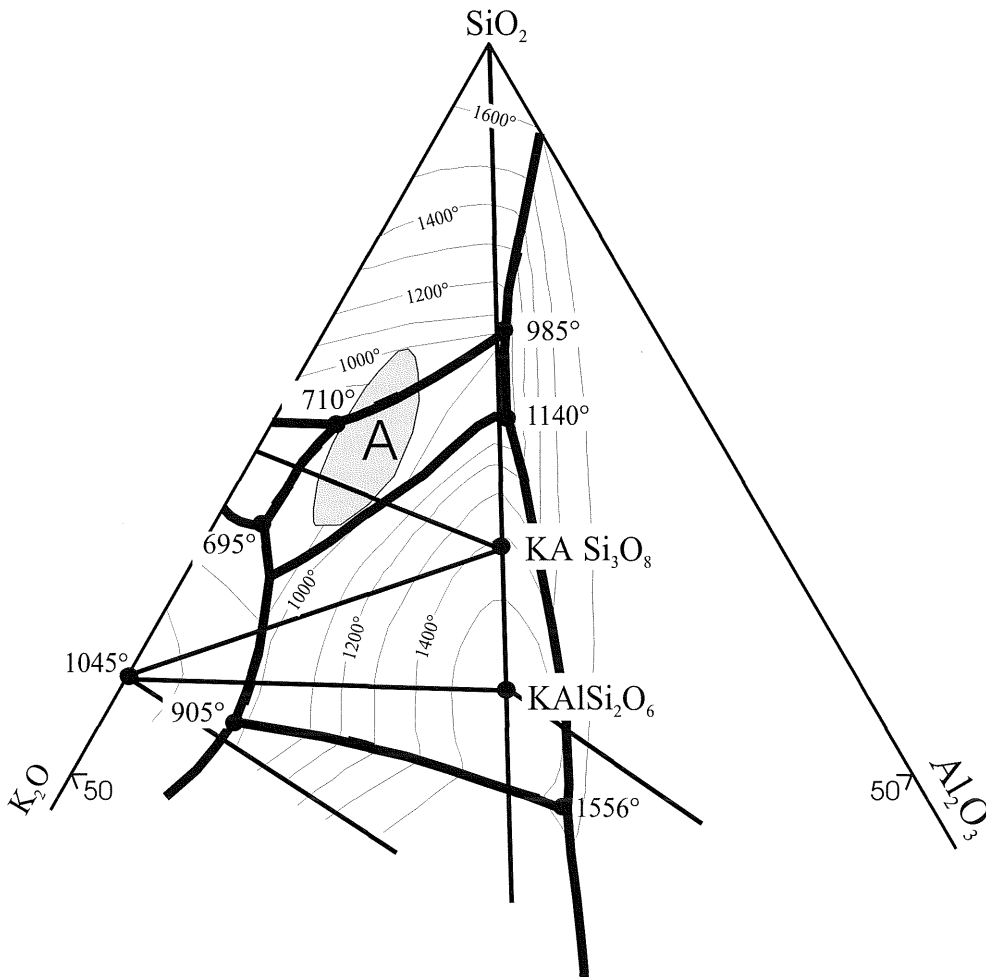


Fig. 7 – Liquidus (heavy lines) and solidus surfaces (light lines) in KAS system (Schairer and Bowen, 1955). A: spot analysis compositions of glass cake.

arrangements of tetrahedral-fold cations ( $\text{SiO}^4$ ,  $\text{AlO}^{3-}$ ) and determines the various properties and features of the glass itself. Differences in viscosity are compositionally determined by polymerisation patterns within different portions of the glass. This means that low effective diffusivity prevents the attainment of homogeneous compositions during glass melting, and evidence of early production steps is consequently retained. Inhomogeneities may

indicate the composition of recycled glass and/or the addition of stabilising components, and may imply poor efficiency in firing technology, preventing homogenisation of the glass melt. In the vitreous mass of Lomello (sample US3358B), enrichment in CaO and a concomitant decrease in  $\text{SiO}_2$ , revealed by the darker layer (spot 9, fig. 2), is compatible with the addition of a Ca-bearing stabilising agent.

Mineral relics in microtextures present in

glassy materials (i.e., fining slag) have important archaeometric value because they allow us to infer the provenance attributes of the raw materials. Moreover, the compositions of relic mineral phases supply important analytical grounds on which to identify the recipes followed during glass making, in terms of vitrifying, stabilising, flushing and additive components. The addition of phosphorus is an expedient used to opacify and whiten glass. Historical documents providing written evidence of the use of plant ash are widespread. Despite this, mineral relics of K-feldspar are found in the Val Gargassa glass samples. The presence of an isotropic phase with K-feldspar composition in the Lomello glass samples (fig. 3C) may be interpreted according to the subliquidus relationships of the KAS system, in which a feldspar-type phase may form during melting by peritectic reaction. This seems to validate statements on the use of plant ash as a supplier of K to the batch. The thermal properties of the batch prevented easy melting, and glass recycling had a catalytic effect.

Parts of the cooling history may be reconstructed from the crystallisation pathway, which is closely connected with under-cooling. As a consequence, the cooling history may reveal particular operations carried out during glass working. Diopside crystals within the vitreous mass (sample US1-VGR11, figs. 4A, 4B) display reabsorption phenomena, compatible with reheating after early cooling.

Together with composition, cooling history plays an important role in identifying the intrinsic properties of glass which, in turn, have deep implications on its durability and conservation.

Present-day archaeometric studies on glass are chiefly devoted to characterising finished artefacts (worked glasses), with the widespread use of bulk chemical analyses. This implies the assumption of the homogeneous composition of glass.

In the archaeometry of glass production, unfinished products with their compositional variability (resulting from spot analyses)

may indicate particular steps in the production cycle and expedients or recipes used during glass melting and/or making. Consequently, study of ancient glass technology requires a multi-disciplinary approach, in which Archaeology and Material Sciences are equally important.

Preliminary, unpublished data on glass from stained windows and worked glass suggest caution in the straightforward application of bulk analyses, because microprobe spot analyses reveal great compositional variations even within a single sample.

#### ACKNOWLEDGMENTS

The authors would like to thank G. Poli (Perugia) and an anonymous reviewer for their fruitful criticism. This work also benefited from stimulating discussions with E. Giannichedda (Genova), T. Mannoni (Genova) and M. Mendera (Siena). This research is supported by MURST-Cofin grant (BM).

#### REFERENCES

- BLAKE H. and MACCABRUNI C. (1985) — *Lo scavo a Villa Maria di Lomello (Pavia) 1984*. *Archeologia Medievale*, XII, 5-28.
- BLAKE H., MACCABRUNI C., PEARCE M. (1987) — *Ricerche archeologiche a Lomello 1984-85*. *Archeologia Medievale*, XIV, 157-87.
- CABLE M. (1991) — *Classical glass technology*. In «*Material Science and Technology*». VCH publishers, New York, 797 pp.
- CAIRO A., MELONI S., MESSIGA B., ODDONE M., RICCARDI M.P. (2001) — *The manufacture of Roman ceramic artifacts in the Po Plain\*\**: a multi-analytical approach. *Revue d'Archéométrie* (submitted).
- CHALMERS B. (1964) — *Principles of solidification*. J. Wiley, New York, 342 pp.
- FOY D. and JÉZÉGOU M.P. (1996) — *Commerce et technologie du verre antique, le témoignage de l'épave Ouest Embiez 1*. In **121** *Congrès National des Sociétés Historiques et Scientifiques*.
- FOY D. and JÉZÉGOU M.P. (1997) — *Une épave chargée de lingots et de vaisselle de verre, un témoignage exceptionnel du commerce et de la technologie du verre en Méditerranée antique*. *Verre*, 3.3, 65-70.

- FOY D., VICHY M., PICON M. (1998) — *Lingots de verre en Méditerranée occidentale (III<sup>e</sup> siècle av. J.C. - VII<sup>e</sup> siècle ap. J.C.)*. In «Annales du 14<sup>e</sup> Congrès de AIHV», 51-7.
- GIANNICCHEDDA E. (1992) — *Per un'Archeologia dei villaggi e delle attività vetrarie in valle Stura*. Archeologia Medievale, XIX, 629-661.
- GIANNICCHEDDA E. (1997) — *Prima campagna di scavo in val Gargassa, località Veirera (Rossiglione, Genova)*. Notiziario di Archeologia Medievale, 69-70, 47.
- GIANNICCHEDDA E., LERMA S., MANNONI T., MESSIGA B., RICCARDI M.P. (2000) — *Archeologia del vetro medievale in Liguria*. In: «Atti Convegno Società Archeologi Medievisti Italiani», Brescia, September 2000
- GOODMAN C.H.L. (1986) — *A new way of looking at glass*. Glass Technology, 28(2), 19-29.
- GRATUZE B., DUSSUBIEUX L. and BOPEARACHCHI O. (1998) — *Etude de perles de verre trouvées au Sri-Lanka, III<sup>e</sup> s. av. J.C. - II<sup>e</sup> s. ap. J.C.: Fabrication locale et importation*. In «Annales du 14<sup>e</sup> Congrès de AIHV», 46-50.
- JACKSON C.M., SMEDLEY J.W., BOOTH C.A., LANE B.C. (1998) — *Biringuccio on 16th century glassmaking*. In «Annales du 14<sup>e</sup> Congrès de AIHV», 335-340.
- LIBOUREL G., STERPENICH J., BARBEY P., CHAUSSIDON M. (1997) — *Caractérisation microstructurale, minéralogique et chimique de l'altération des vitraux*. In «Les matériaux vitreux: verre et vitraux», Edipuglia s.r.l, Bari, 75-89.
- MANNONI T. and GIANNICCHEDDA E. (1996) — *Archeologia della produzione*. Einaudi, Torino, 352 p.
- MORETTI C. and MORETTI S. (1998) — *Le materie prime dei vetrai veneziani: natura, lessico e fonti di approvvigionamento rilevate nei ricettari dal XIV al XIX secolo*. In «Annales du 14<sup>e</sup> Congrès de AIHV», 21-2.
- NENNA M.D., VICHY M., PICON M. (1997) — *L'atelier de verrier de Lyon du 1<sup>er</sup> siècle après J.C. et l'origine des verres «romains»*. Revue d'Archéométrie, 21, 81-7.
- NEWTON R.G. (1980) — *Recent views on ancient glasses*. Glass Technology, 21, 173-183.
- NEWTON R., DAVIDSON S. (1997) — *Conservation of glass*. Butterworth-Heinemann Series in Conservation and Museology, Linacre House, Oxford, 286 pp.
- OPPENHEIM A.L., BRILL R.H., BARAG D., VON SALTERN A. (1970) — *Glass and glassmaking in ancient Mesopotamia*. Corning Museum of Glass, New York, 104 pp.
- ROEDDER E., (1979) — *Silicate liquid immiscibility in magmas*. In «The Evolution of Igneous Rocks: Fiftieth Anniversary Perspectives», Princeton. Princeton University Press, pp. 483-520.
- SCHAIRES J.F. and BOWEN N.L., (1955) — *The system K<sub>2</sub>O-Al<sub>2</sub>O<sub>3</sub>-SiO<sub>2</sub>*. Am. J. Sci., **253**, 681-746.
- SCHWOERER M., DUBERNET S., RAFFAILLAC-DESFOSSÉ C., BECHTEL F. (1997) — *Sur l'altération des verres anciens: vitraux, objets en verre et glacures*. In «Les matériaux vitreux: verre et vitraux», (Ed.), Edipuglia s.r.l, Bari, 91-105.
- STERNINI M. (1995) — *La fenice di sabbia. Storia e tecnologia del vetro antico*. Edipuglia s.r.l, Bari, 217 p.
- UHLMANN D.R. and KOLBECK A.G. (1976) — *Phase separation and the revolution in concepts of the glass structure*. Phys. Chem. Glass, 17,147-157.
- ZACHARIASEN W.H. (1932) — *The atomic arrangement in glass*. J. Am. Chem. Soc., 54, 3841-51.